

## *Supplemental Information for*

# **Giant Manipulation of Thermal Conductivity Anisotropy in Black Phosphorene Under External Electric Fields**

Zhonghua Yang<sup>1,\*</sup>, Mengyuan Zhang<sup>1</sup>, Wen Gu<sup>1</sup>, Xinyi Xu<sup>1</sup>, Chan Liu<sup>2</sup>, Xinying  
Lan<sup>1</sup>

<sup>1</sup>School of Architecture and Civil Engineering, Shenyang University of Technology,  
Shenyang, 110870, China

<sup>2</sup>Academy of Science and Technology, Shenyang University of Technology,  
Shenyang, 110870, China

The atomic displacement, dipole moment, and structural energy variation as a function of the external electric field's intensity are depicted in **Figure S1**. In **Figure S1(a)**, the displacement of the phosphorus atom (P) remains largely invariant until the external electric field surpasses a threshold of  $E_{(f,xx)} = 0.05 \text{ V/\AA}$ , beyond which all structural parameters exhibit an exponential increase relative to the electric field strength. At an electric field of  $E_{(f,xx)} = 0.2 \text{ V/\AA}$ , the displacement of the P atom is marginally altered by  $4.2 \times 10^{-7} \text{ \AA}$ , indicating that the buckled configuration of black phosphorene is maintained robustly. Consequently, this correspondence disregards variations in structure induced by differing electric fields. Moreover, **Figure S1(b)** illustrates a linear escalation in the dipole moment with increasing electric field intensity. Furthermore, as the electric field strength intensifies, the total energy of black phosphorene diminishes, corroborating a thermodynamically more stable structure under external influence, which forms the foundational basis for subsequent phonon transport calculations, as referenced in **Figure S1(c)**.

---

\* Author to whom all correspondence should be addressed. E-Mail: [yang@sut.edu.cn](mailto:yang@sut.edu.cn) ( Z.Y.)

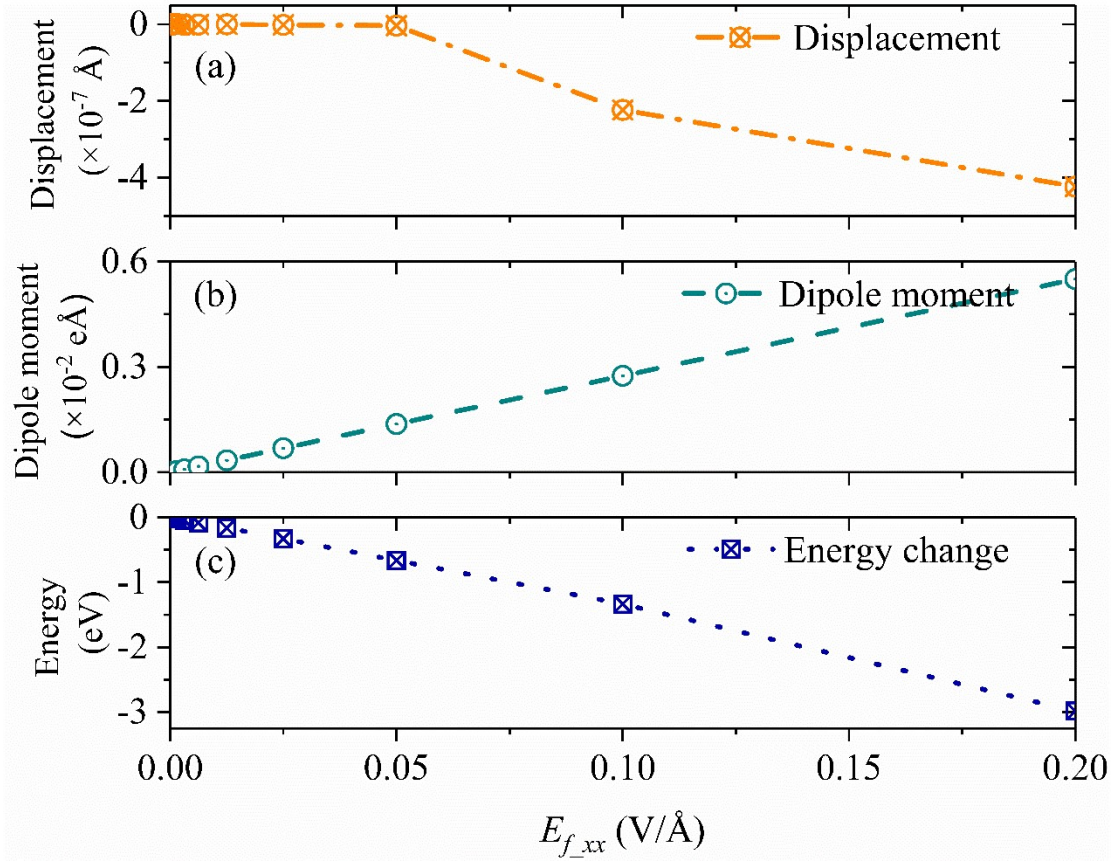


**Figure S1.** The changes of (a) atomic displacement (b) dipole moment (c) structural energy as a function of the strength of *Zigzag* electric field.

The phonon transport characteristics of black phosphorene are assessed utilizing the ShengBTE computational package<sup>[1]</sup>. The requisite second-order (harmonic) and third-order (anharmonic) interatomic force constants (IFCs) are determined via the method known as compressive sensing lattice dynamics (CSLD)<sup>[2]</sup>. An exhaustive analysis of the thermal conductivity's convergence concerning the cutoff energy and *Q-grid* is presented in **Figure S2**. As depicted in **Figure S2(a)**, with an increment in the cutoff energy, the structural energy initially decreases and subsequently stabilizes beyond a threshold of 50 Ry. Similarly, **Figure S2(b)** illustrates that the thermal conductivity of black phosphorene exhibits a well-converged profile once the *Q-grid* exceeds dimensions of  $50 \times 50 \times 1$ . Consequently, to balance computational efficiency and accuracy, the cutoff energy is established at 50 Ry and the *Q-grid* configuration at  $50 \times 50 \times 1$  for subsequent calculations of thermal conductivity.

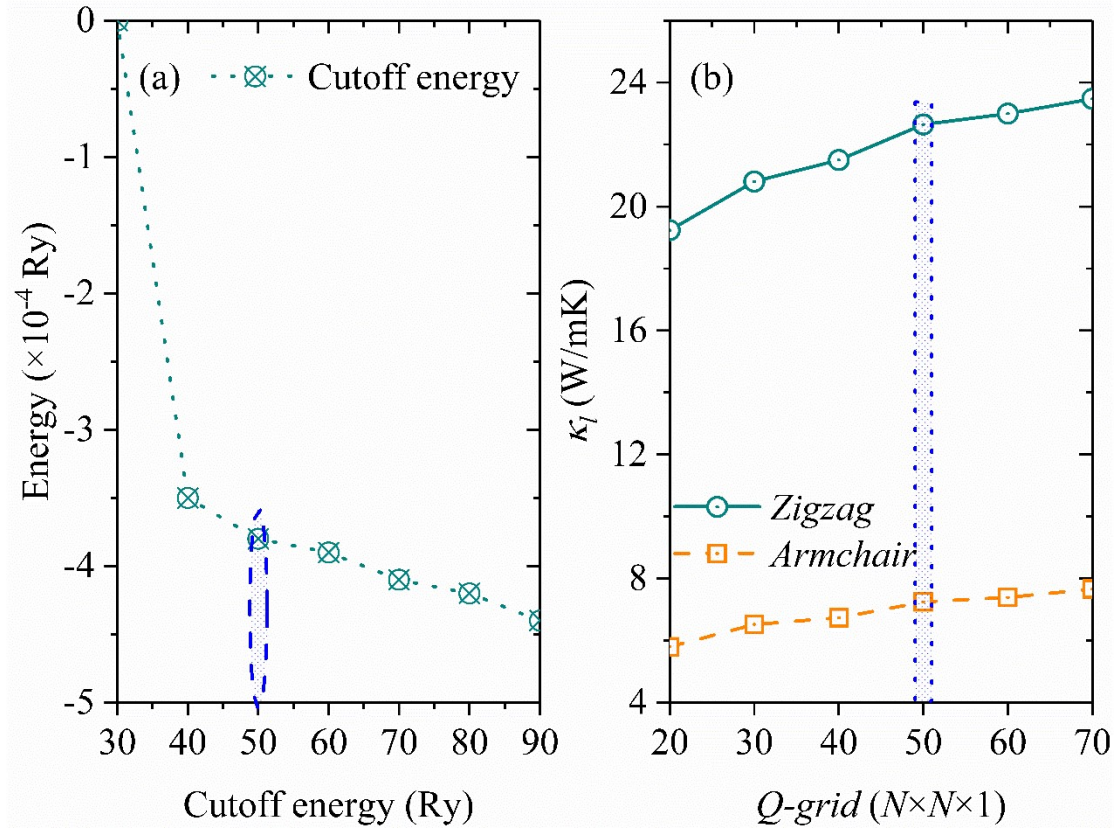


**Figure S2.** (a) The structure energy as a function of cutoff energy. (b) The thermal conductivity as a function of  $Q$ -grid.

The differential charge density (DCC) of black phosphorene under representative electric fields is depicted in **Figure S3**. A comparative analysis between **Figure S3(a)** and **Figure S3(b)** reveals that the electric field induces a positive accumulation and a negative depletion of charges, leading to induced charges of opposite signs localized around the phosphorus cores. In **Figure S3(c)**, with an applied electric field of  $E_{(f_{yy})} = 0.2$  V/Å, there is a redistribution of charges along the *Armchair* direction, with a reduction in the number of ionic bonds compared to the configuration under  $E_{(f_{xx})} = 0.2$  V/Å. Consequently, there is a minimal alteration in the lifetime and anisotropic thermal conductivity of black phosphorene. The DCC isosurface set at  $1 \times 10^{-5}$  (a.u.) in **Figure S3(d)**, significantly smaller than in other configurations, indicates a lesser induction of charges by  $E_{(f_{zz})} = 0.2$  V/Å. This observation is consistent with a charge accumulation at the bottom of the lower plane and a depletion at the top of the upper plane, aligning

with findings reported in the previous reference<sup>[3]</sup>.

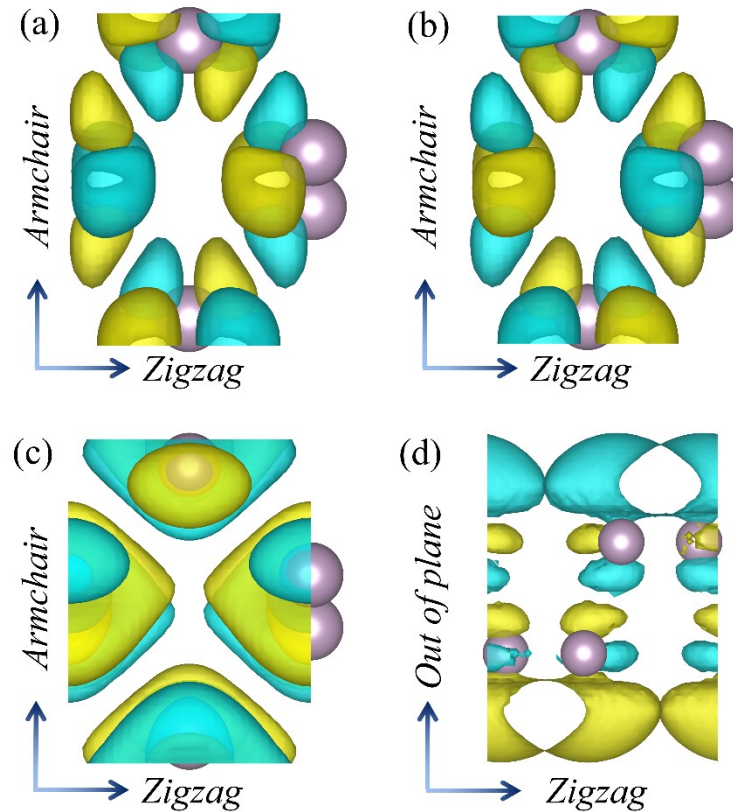


**Figure S3.** Top view of the charge density (yellow, positive; cyan, negative) under the electric field of (a)  $E_{(f_{xx})} = 0.2 \text{ V/\AA}$ , (b)  $E_{(f_{xx})} = -0.2 \text{ V/\AA}$ , (c)  $E_{(f_{yy})} = 0.2 \text{ V/\AA}$ . The isosurface is set as  $1 \times 10^{-4}$  (a.u.). (d) Side view of the charge density under the electric field of  $E_{(f_{zz})} = 0.2 \text{ V/\AA}$ . The isosurface is set as  $1 \times 10^{-5}$  (a.u.).

### Reference:

- [1] Li W, Carrete J, Katcho N, Mingo N. ShengBTE: A solver of the Boltzmann transport equation for phonons. *Computer Physics Communications*, 2014, 185: 1747–1758.
- [2] Zhou F, Nielson W, Xia Y, Ozoliņš V. Lattice Anharmonicity and Thermal Conductivity from Compressive Sensing of First-Principles Calculations. *Physical Review Letters*, 2014, 113(18): 185501.
- [3] Wang X-P, Li X-B, Chen N-K, Zhao J-H, Chen Q-D, Sun H-B. Electric field analyses on monolayer semiconductors: the example of InSe. *Physical Chemistry Chemical Physics*, 2018, 20(10): 6945-6950.